

Three years of Atmospheric Infrared Sounder radiometric calibration validation using sea surface temperatures

H. H. Aumann,¹ Steve Broberg,¹ Denis Elliott,¹ Steve Gaiser,¹ and Dave Gregorich¹

Received 26 October 2005; revised 1 March 2006; accepted 18 April 2006; published 23 August 2006.

[1] This paper evaluates the absolute accuracy and stability of the radiometric calibration of the Atmospheric Infrared Sounder (AIRS) by analyzing the difference between the brightness temperatures measured at 2616 cm^{-1} and those calculated at the top of the atmosphere (TOA), using the Real-Time Global Sea Surface Temperature (RTGSST) for cloud-free night tropical oceans between $\pm 30^\circ$ latitude. The TOA correction is based on radiative transfer. The analysis of the first 3 years of AIRS radiances verifies the absolute calibration at 2616 cm^{-1} to better than 200 mK, with better than 16 mK/yr stability. The AIRS radiometric calibration uses an internal full aperture wedge blackbody with the National Institute of Standards and Technology (NIST) traceable prelaunch calibration coefficients. The calibration coefficients have been unchanged since launch. The analysis uses very tight cloud filtering, which selects about 7000 cloud-free tropical ocean spectra per day, about 0.5% of the data. The absolute accuracy and stability of the radiometry demonstrated at 2616 cm^{-1} are direct consequences of the implementation of AIRS as a thermally controlled, cooled grating-array spectrometer and meticulous attention to details. Comparable radiometric performance is inferred from the AIRS design for all 2378 channels. AIRS performance sets the benchmark for what can be achieved with a state-of-the-art hyperspectral radiometer from polar orbit and what is expected from future hyperspectral sounders. AIRS was launched into a 705 km altitude polar orbit on NASA's Earth Observation System (EOS) Aqua spacecraft on 4 May 2002. AIRS covers the 3.7–15.4 micron region of the thermal infrared spectrum with a spectral resolution of $\nu/\Delta\nu = 1200$ and has returned 3.7 million spectra of the upwelling radiance each day since the start of routine data gathering in September 2002.

Citation: Aumann, H. H., S. Broberg, D. Elliott, S. Gaiser, and D. Gregorich (2006), Three years of Atmospheric Infrared Sounder radiometric calibration validation using sea surface temperatures, *J. Geophys. Res.*, *111*, D16S90, doi:10.1029/2005JD006822.

1. Introduction

[2] The Atmospheric Infrared Sounder (AIRS) is a grating-array spectrometer which covers the 3.7–15.4 micron spectral region with 2378 spectral channels and nominal spectral resolution of $\nu/\Delta\nu = 1200$. The objective of this paper is to validate the absolute AIRS radiometric calibration at a level better than the 200 mK prelaunch expected absolute accuracy, and to evaluate the stability of the calibration at a level approaching the canonical 10 mK/yr value of global warming.

[3] AIRS was designed to support the near real-time requirements of the numerical weather prediction centers for global temperature and moisture soundings and NASA's climate research program [Aumann *et al.*, 2003]. For the purpose of soundings alone, cooling of the detector arrays to 58 K by itself would have more than sufficed to achieve the required sensitivity. The application of the data to climate

research and the expected, and since 2004 de facto, use of AIRS as an operational sounder in support of weather forecasting made additional demands on the traceability and stability of the calibration. This was accomplished for AIRS with additional design features and additional prelaunch testing. The AIRS On-board Blackbody Calibrator (OBC) is a full aperture wedge-shaped cavity. The wedge design and Aeroglaze Z302 coatings produce an effective emissivity of better than 0.999. The OBC is maintained at a constant temperature, nominally 308.2 K. The actual OBC temperature, derived from four independent resistance thermometers, shows a seasonal 10 mK variation between 308.18 K and 308.19 K, which is included in the calibration. The entire spectrometer is cooled to 156 K and maintained to within 30 mK of its set point. Extensive prelaunch radiometric calibration of AIRS at a number of optical bench temperatures and scan angles using a NIST-certified blackbody showed that the AIRS radiometric calibration was accurate to within 200 mK for uniformly illuminated scenes between 220 K and 320 K [Pagano *et al.*, 2003]. Near 300 K, the typical temperature of tropical oceans, most of the absolute calibration uncertainty comes from the uncertainty in the effective emissivity of the OBC.

¹Jet Propulsion Laboratory, California Institute of Technology, Pasadena, California, USA.

The OBC blackbody gain correction factor, derived from the NIST calibrated secondary standard, was 1.000 ± 0.002 owing to the combined effects of all system components. This is equivalent to a one sigma uncertainty of 0.002 in the effective OBC emissivity. For a 300 K scene the emissivity uncertainty of 0.002 introduces a wave number dependent uncertainty in the absolute calibration, 48 mK RMS at 2616 cm^{-1} and 101 mK RMS at 1231 cm^{-1} . The wave number dependence is due to the slope of the Planck function. The AIRS radiometric calibration uses the NIST traceable prelaunch calibration coefficients and has been unchanged since launch. However, long-term exposure of the instrument, including the OBC temperature sensors, to high-energy radiation and molecular contamination of surfaces may degrade the accuracy of the calibration with time. While the AIRS design may have helped to push many of these effects below second-order terms, the ultimate verification of accuracy and stability has to come from the observations of bona fide external standards.

[4] As a consequence of the grating-array spectrometer design, the 2378 AIRS channels operate as simple, independent radiometers which share the OBC and space views, each using the same calibration software, but each with their own prelaunch determined calibration coefficients. In principle, it is therefore only necessary to validate the absolute accuracy and stability of the OBC with one channel to establish the radiometric accuracy and stability of all channels. The AIRS design gives us the flexibility to select the simplest channel. We use three years of AIRS data to validate the prelaunch expectations of absolute calibration accuracy and stability using the most accessible bonafide external standard, the tropical ocean sea surface temperatures (SST).

2. Approach

2.1. Overview

[5] In principle, there are several ways to accomplish the validation of the accuracy of the calibration of an infrared radiometer in Earth orbit using independent measurements of the SST. In all cases the validation is based on the statistical analysis of the difference between the observed brightness temperatures (obs) and those calculated (calc) at the top of the atmosphere (TOA). The challenge for accomplishing this with better than 200 mK absolute accuracy using the SST is the difficulty of making the TOA atmospheric corrections at the required level of accuracy, aggravated by the virtual omnipresence of clouds. A number of validation approaches were considered before the launch of AIRS [Hagan and Minnett, 2003] (hereinafter referred to as HM2003) using the SST. HM2003 considered matchups with buoys, matchups with surface observations from MAERI, a ship-mounted radiometer [Minnett *et al.*, 2001] and matchups with mapped products. Each approach has its own advantages and disadvantages when applied to AIRS data. We elected to pursue the matchup with a mapped product.

[6] Fixed and floating buoys have for many years been the foundation of the most direct and accurate measurements of the SST. The buoys are calibrated with NIST traceability by the vendors to about 0.1 K (HM2003) and are replenished on a regular basis. Buoy matchups and

matchups with mapped products both refer to the temperature at about one meter below the surface. The difference between the skin temperatures is of the order of 0.2 K with some uncertainty. This will be discussed later in this paper. The problem with using buoy measurements for the validation is the very low yield of clear matchups due to cloud contamination. HM2003 assumed that 10–20% of the buoys observations would report under cloud-free conditions, with the expectation of a robust buoy matchup data set in 30 days. While this estimate may be appropriate to the 1 km footprint of an AVHRR, AATSR, or MODIS type radiometer, it was recognized fairly quickly [Aumann, 2003] that less than 1% of the AIRS 15 km ocean footprints could be considered adequately free of clouds at the level of accuracy demanded for absolute calibration validation at the 200 mK level. As a consequence of the very low yield, the buoy matchup analysis was not pursued. The MAERI surface measurements are most directly comparable to the AIRS surface skin temperature measurements. There are only a few MAERI operationally deployed, so yield for MAERI matchups is 2 orders of magnitude lower than for buoy matchups.

[7] Mapped SST products are generated by time and space interpolating the buoy measurements to create a uniformly spaced global grid of measurements. Matchups with the mapped SST products under cloud-free conditions produce a strong database: If 1% of ocean footprints are identified as cloud free, each daily matchup file contains about 10,000 entries. There are a number of mapped SST products, including the Reynolds SST [Reynolds *et al.*, 2002], available weekly on a 1° grid, and the higher-resolution Real Time Global SST [Thiébaux *et al.*, 2003], hereinafter referred to as RTGSST, which is produced daily on a half-degree latitude/longitude grid. We selected the RTGSST product for the validation of the AIRS radiometric calibration presented in this paper. The RTGSST was developed by the National Centers for Environmental Prediction/Marine Modeling and Analysis Branch (NCEP/MMAB) in support of daily weather forecasting. It uses two-dimensional variational interpolation of buoy and ship surface temperature measurements and satellite-retrieved SST data from the previous day. The RTGSST is readily available from <http://polar.ncep.noaa.gov/sst/> for near-real-time processing and is used as the daily input to the numerical weather forecasting by NCEP and the European Center for Medium-range Weather Forecasting (ECMWF). With its 0.5° grid, the nearest matchup point is always within 35 km. For the AIRS 15 km (at nadir) footprint and statistical analysis, selecting the closest grid point introduces no significant interpolation bias error.

[8] The RTGSST is daily quality-controlled by NCEP/MMAB. For the highest absolute accuracy we limited our analysis to the tropical oceans within 30° of the equator, which is rich in buoys. The root mean square deviation (rmsd) relative to the tropical verification buoys (i.e., buoys held back from the assimilation into the RTGSST) is typically between 0.45 K and 0.55 K. For large area averages, such as the tropical oceans, the absolute accuracy and stability of the RTGSST products should considerably exceed the absolute 0.1 K accuracy of the individual buoys. The statistical bias relative to the verification buoy set shows small seasonal trends, but the day/night averaged

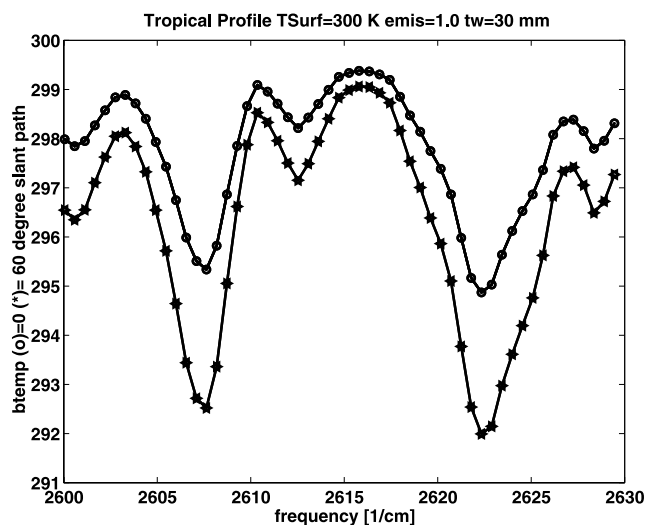


Figure 1. Calculated spectrum of tropical night ocean between 2600 and 2630 cm^{-1} for $T_{\text{Surf}} = 300 \text{ K}$ and 30 mm precipitable water at nadir (starred line) and 60° local zenith angle (dotted line). The window channel at 2616.3 cm^{-1} and the water sensitive channel at 2607.8 cm^{-1} are used for the derivation of sst2616.

bias has been within 50 mK of zero since September 2002, when AIRS operational data gathering started, through August 2005, the most recent data used in this paper.

[9] In the following, we discuss details of how the AIRS data were selected, the atmospheric and emissivity corrections, and the bias introduced by comparing daily mean bulk temperatures from the RTGSST to night skin temperatures. In all cases we estimate the size of expected bias and bias uncertainty.

2.2. AIRS Data

[10] Each day the AIRS spectrometer generates 2.9 million spectra globally, corresponding to about 36 GBytes of calibrated radiances. The AIRS Calibration Data Subset (ACDS) is a 30 Mbyte per day subset of the AIRS data created in support of the efficient near-real-time validation and long-term trend analysis of the AIRS calibration. Most of the data saved in the ACDS are from first-pass cloud-screened nonpolar ocean footprints. For these footprints 84 of 2378 AIRS channels, 15 Advanced Microwave Sounding Unit (AMSU) channels [Lambrigtsen, 2003] and three of the four AIRS Vis/NIR channels [Gautier *et al.*, 2003] are saved. An AIRS footprint is defined as “first-pass cloud-free” if it passes a spatial coherence test [Coakley and Bretherton, 1982] and a simple low stratus cloud test. The spatial coherence test uses 3×3 groups of AIRS footprints. The spatial coherence parameter, cx2616, is defined as the difference between the maximum and the minimum brightness temperatures at 2616.3 cm^{-1} of a 3×3 group. If cx2616 is below the threshold of 1.2 K, the center footprint is defined as likely cloud free. The low stratus test [Aumann *et al.*, 2004] makes use of the fact that the atmosphere above stratus clouds is very dry. This dry layer can be detected directly from the water vapor sensitive channels in the AIRS spectrum. The same cloud filter is used day and night, typically identifying 100,000 of the two million ocean

spectra from one day, i.e., about 5%, as reasonably clear. The information from the Vis/NIR channels is held back for diagnostics, as will be discussed later in this paper. For the calibration validation presented in the following, the data were rescreened:

[11] 1. We used a tighter spatial coherence threshold of 0.5 K and additional spectral filtering, including a lapse rate test [Aumann *et al.*, 2004], to identify the most cloud-free spectra.

[12] 2. In order to limit the data to the area where the RTGSST is most accurate, as discussed earlier, the data was limited to the tropical oceans within 30° from the equator. The resulting surface temperatures are in the 295–305 K range.

[13] 1. In order to simplify the emissivity correction, as discussed later in the paper, we eliminated data with satellite zenith angles larger than 35° . Although this eliminates almost 50% of the scanned area, it eliminates only about 25% of the clear spectra, since the number of spectra identified as clear at the larger zenith angles drops off due to the combination of cloud thickness effects and the larger footprints compared to nadir.

[14] This rescreening reduced the number of available cloud-free spectra to about 7000 per day, corresponding to about 0.5% of all tropical ocean footprints. The number of footprints from the ascending (day) and the descending (night) portions of the orbits are roughly equal.

2.3. Atmospheric Absorption and Emissivity Corrections

[15] The AIRS radiometric validation is based on the statistical analysis of the difference between the observed brightness temperatures and those calculated at the top of the atmosphere (TOA) using the RTGSST. The smaller the absorption, the more accurate the TOA calculation. Earlier we pointed out that with the AIRS grating-array design it is only necessary to validate the absolute accuracy and stability of the OBC with one channel to establish the accuracy and stability of all channels. For this validation we select the 2616.3 cm^{-1} channel, which is the most transparent channel in the AIRS spectrum [Chahine, 1981]. Figure 1 shows the 2600 to 2630 cm^{-1} region of the AIRS spectrum under tropical conditions (30 mm precipitable water) at nadir and for a 60° satellite zenith angle. At nadir there is only about 0.3 K of absorption at 2616.3 cm^{-1} : 0.16 K due to water vapor continuum, about 0.07 K due to nitrogen continuum, and 0.06 K due to other minor gases, mostly methane and some carbon dioxide. Table 1 lists the atmospheric correction at nadir at 2616.3 cm^{-1} and the next best window channel, 1231 cm^{-1} , for 30 mm precipitable water, typical of clear night tropical ocean, using the Radiative Transfer Algorithms (RTA) provided by Strow *et al.* [2003]. At 1231 cm^{-1} , a channel that will be used later in the paper, there is 1 order of magnitude more absorption due to water vapor continuum. The Noise equivalent Delta Temperature (NeDT) applicable to each channel when viewing a 300 K source is 0.1 K or smaller (Table 1, last column), typical of all channels in this area of the spectrum. Low random noise is key for the reliable identification of cloud-free spectra.

[16] The radiometric calibration validation is based on the analysis of (obs-calc). The TOA-calculated brightness temperature at 2616.3 cm^{-1} uses the RTGSST, corrected for

Table 1. Comparison of the Window Channels Available From AIRS, Showing That the 2616 cm^{-1} Window Channel is by Far the Most Transparent

Channel Wave Number	Required Correction at 30 mm Precipitable Water	NeDT at 300 K
2616	0.29 K	0.08 K
1231	1.6 K	0.05 K

water vapor absorption, A2616, and emissivity, E2616; that is, $\text{calc} = \text{RTGSST} - \text{A2616} - \text{E2616}$. This equation is symbolic, since strictly speaking the emissivity correction is not additive, but has to be done in the radiance domain. If we define $\text{sst2616} = \text{bt2616} + \text{A2616} + \text{E2616}$ as the skin temperature, then the analysis of $(\text{obs} - \text{calc}) = (\text{bt2616} - \text{RTGSST} + \text{A2616} + \text{E2616})$ can be stated as $(\text{obs} - \text{calc}) = (\text{sst2616} - \text{RTGSST})$. We prefer to discuss the validation in terms of $(\text{sst2616} - \text{RTGSST})$, because its meaning is more intuitive, but numerically it is equivalent to $(\text{obs} - \text{calc})$. The bias introduced by the fact that the RTGSST is not the skin temperature, but the daily mean temperature at about one meter below the surface, is discussed later in this paper.

2.3.1. A2616

[17] The atmospheric transmission correction, A2616, is variable owing to the variability of the water vapor. We note from Figure 1 that with increasing amount of water vapor in the slant path there is a corresponding increase in the difference between the brightness temperature at 2616.3 cm^{-1} and at 2607.8 cm^{-1} . While the atmospheric absorption at 2616.3 cm^{-1} window channel is typically 0.3K, the absorption at 2607.8 cm^{-1} is typically 3 K. The opacity in the 2607.8 cm^{-1} channel is due to unresolved weak water lines. We define $q_2 = (\text{bt2616} - \text{bt2607})$, where bt2616 and bt2607 are the observed brightness temperatures at 2616 and 2607 cm^{-1} , respectively. If T_{surf} is the surface skin temperature (assuming unity emissivity), then $\text{A2616} = T_{\text{surf}} - \text{bt2616}$ is the transmission loss due to the atmospheric absorption. Figure 2 shows $T_{\text{surf}} - \text{bt2616}$ calculated for 24 profiles with surface temperature greater than 270 K at six slant path angles from nadir to 50° , i.e., a total of 144 cases, as function of q_2 . At $q_2 = 0$ the absorption of 0.13 K is due to nitrogen, methane, and carbon dioxide. The absorption for all slant paths is plotted on this graph; that is, at the larger slant paths there is more water absorption and q_2 increases correspondingly. The calculation of q_2 from the spectrum then gives the required atmospheric transmission correction. The computation of A2616 uses a quadratic fit through the model atmospheres, which fits the data with 0.05 K rms.

[18] There is an uncertainty in A2616. For the evaluation of the uncertainty in the atmospheric absorption due to uncertainties in the spectral response characterization, we replaced the AIRS RTA (which uses the MT-CKD water continuum) with a line-by-line calculation. We then repeated the calculation, but replaced the prelaunch calibrated AIRS spectral response function with simple triangular spectral response functions with $\nu/1200$ full width at half peak. The absorption for the tropical atmosphere changed by less than 0.01 K. In the RTA validation paper [Strow *et al.*, 2006] the estimated uncertainty of the absorption at 2616 cm^{-1} due to all active gases is stated as $-0.04 \pm$

0.08 K. We use this estimate as the formal bias and bias uncertainty in A2616.

2.3.2. E2616

[19] For the emissivity correction, E2616, we use the scan angle and wind speed dependent seawater emissivity from Masuda *et al.* [1988]. The emissivity used in the calculations is based on a numerical fit to the Masuda data as a function of scan angle at 5 m/s wind speed, close to the 7 m/s from tropical ocean climatology. In order to avoid uncertainties associated with emissivity and wind speed effects at the zenith angles larger than 40° , we limited the AIRS data used for this paper to zenith angles less than 35° . This choice eliminates 28% of the clear spectra in return for a much tighter emissivity uncertainty estimate. We use the 0.0015 mean difference in the emissivity between the 5 m/s and 10 m/s Masuda values for zenith angles between zero and 35° as an estimate of a potential emissivity uncertainty. This is equivalent to a bias uncertainty of 0.03 K (for a 290 K surface) in the emissivity correction.

2.4. RTGSST Bias

[20] The 2616 cm^{-1} measurements refer to the temperature within 0.1 mm of the sea surface, while the buoys, which are used as the primary reference for the RTGSST, are located about one meter below the surface. In addition, the RTGSST refers to the daily mean buoy temperature, while the AIRS measurements are made at the time of the overpasses near 1:30 AM and 1:30 PM local time. In order to properly interpret results obtained from using the RTGSST to calculate the expected TOA brightness temperatures at the 1:30 AM overpass, we have to apply corrections for the skin/buoy gradient and the day/night bias.

2.4.1. Skin/Buoy Gradient

[21] The skin is typically cooler than the buoys by a wind speed, boundary layer temperature, and water vapor dependent amount. Donlon *et al.* [2002] used a ship-mounted 11 micron radiometer to measure the difference between buoy temperatures and the skin temperature. The skin was

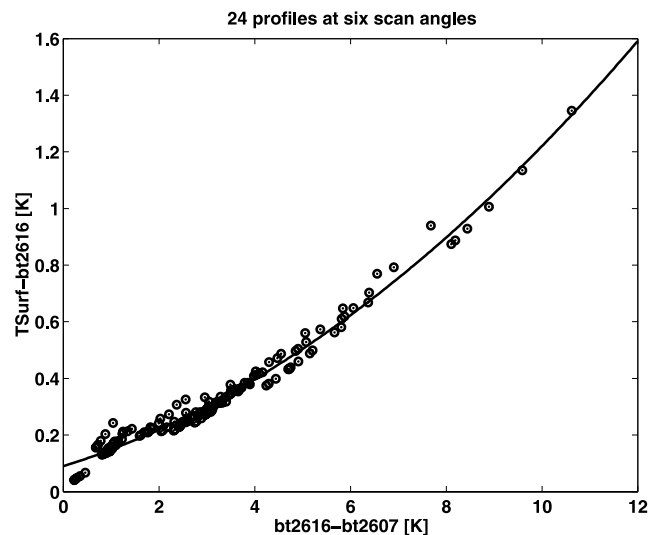


Figure 2. The transmission correction at 2616 cm^{-1} , using $q_2 = \text{bt2616} - \text{bt2607}$ based on 24 profiles for nonfrozen ocean and six satellite zenith angles. The quadratic fits the points with 50 mK standard deviation.

Table 2. (sst1231 – RTGSST) Day and Night Bias as a Function of Cloud Filter Threshold^a

cx2616 Threshold	Night sst1231 – RTGSST	Day sst1231 – RTGSST	Day- Night Bias	Mean vis3, watt m ⁻² μ ⁻¹ sr ⁻¹
0.7 K	–0.64 K	–0.22 K	0.42 K	6.8
0.5 K	–0.59 K	–0.20 K	0.38 K	6.6
0.5 K + vis3 < 5	na	+0.10 K	na	4.7

^aThe addition of the vis3 < 5 filter provides the numerical estimate of cloud contamination.

0.17 K cooler than the buoys, with 0.07 K standard deviation of the individual measurements. There was a wind speed dependence for wind speeds > 6 m/s, but essentially no day/night dependence. For a large number of observations confined to the tropical oceans, the uncertainty in the mean is much smaller than the standard deviation. We use half the standard deviation, 0.03 K, as a very conservative estimate of the bias uncertainty.

2.4.2. Day/Night Bias

[22] The RTGSST represents a day/night average of the buoy temperatures, while the AIRS measurements occur at the local time of the satellite overpasses at 1:30 AM and 1:30 PM. Hourly measurements of buoy temperatures by *Weller and Anderson* [1996] show the top one meter layer of the ocean warming from a minimum near sunrise at 6 AM local time, peaking at 1 PM and then cooling down again. The AIRS measurements occur very close to the daily peak at the 1:30 PM daytime overpasses. At the 1:30 AM night overpasses the surface is less than 50 mK warmer than the daily minimum. We can estimate the day/night bias of the RTGSST relative to the buoys by measuring day/night difference temperatures, $\Delta = \text{SST.day} - \text{SST.night}$. At the 1:30 AM overpass the buoy temperature, $T_{\text{buoy.am}} = \text{RTGSST} - (\Delta - 50 \text{ mK})/2$, while during the 1:30 PM overpass $T_{\text{buoy.pm}} = \text{RTGSST} + (\Delta + 50 \text{ mK})/2$. The 2616 cm⁻¹ channel cannot be used to make accurate daytime measurements, owing to its sensitivity to solar reflected light. For the daytime measurements we use the 1231 cm⁻¹ and 1227 cm⁻¹ channels to create sst1231 [Aumann et al., 2004]. The 1231 cm⁻¹ channel is a relatively good window channel and the difference between it and the 1227 cm⁻¹ channel is used for the water vapor correction, similar to using 2616.3 cm⁻¹ and 2607.8 cm⁻¹. For our particular application, we are interested in obtaining an sst1231 that is the radiometric equivalent to the sst2616 at night. This was accomplished by training sst1231, i.e., determining the coefficient used to express sst1231 in terms of bt1231 and bt1227, on the sst2616 calculated for cloud-free night tropical ocean data from all of October 2003. On the basis of the analysis of all tropical ocean cx2616 = 0.5 K clear night data for the past 3 years, sst2616 and sst1231 agree within $-30 \pm 33 \text{ mK}$. Details of sst1231 algorithm are given in Matlab code in Appendix A.

[23] Since the cloud-free spectra for the descending (night) orbits come from different positions than those for the ascending (day) orbits, we form double differences. We define $d1231 = \text{sst1231} - \text{RTGSST}$, and evaluate $\Delta = \text{mean}(d1231.\text{night}) - \text{mean}(d1231.\text{day})$. Table 2 summarizes the result based on the analysis of 24 days of data, every 48th day between September 2002 and 2005. In order

to get an estimate of the stability of this procedure, we show the change for cx2616 thresholds at 0.7 K and 0.5 K. As the threshold (Table 2, first column) is made tighter, the night bias (second column) and the day bias (third column) both decrease, but the day/night difference (fourth column) is reasonably stable. The cx2616 = 0.5 K filtered data have a mean $\Delta = 0.38 \text{ K}$. We conclude that the buoys at 1:30 AM overpass are $0.38/2 - 0.025 = 0.17 \text{ K}$ colder, during the day they are $0.38/2 + 0.025 = 0.21 \text{ K}$ warmer than the RTGSST. Our derivation of the day/night difference results in a peak-to-peak amplitude of $0.38 + 0.05 = 0.385 \text{ K}$, in agreement with the measurements of *Weller and Anderson* [1996], who conclude that under typical tropical ocean conditions the peak buoy temperature oscillates 0.2 K about the daily mean.

[24] We base the uncertainty of the mean day/night bias on the observation of *Weller and Anderson* [1996] that at 1:30 AM the buoys are typically less than 50 mK warmer than the daily minimum, and use that amount as an estimate of the day/night bias uncertainty. The resulting night bias estimate is then $-0.17 \text{ K} \pm 0.05 \text{ K}$. In splitting the day/night difference we also assumed that the day clouds and night clouds affect the cloud filter equally. The validity of this assumption will be argued in the next section.

2.5. Cloud Contamination: Bias and Bias Uncertainty

[25] The presence of undetected clouds in the “clear” footprints results in a cold bias. In order to estimate this bias we again use daytime measurements with sst1231 and make use of the AIRS visible channel number 3, vis3. The vis3 channel [Gautier et al., 2003] spatially overlays the 15 km IR footprint and covers the 0.75–0.90 micron spectral range, equivalent to the AVHRR vis channel 2. Under perfectly calm cloud-free conditions the tropical ocean is very dark and $\text{vis3} = 4 \text{ watt/m}^2/\mu\text{sr}$. This value increases to $\text{vis3} = 260$ under full overcast (but not glint) conditions. For the estimate of the cloud contamination, we evaluate the correlation between $d1231 = \text{sst1231} - \text{RTGSST}$, the cx2616 threshold, and the signal from the AIRS vis3 channel. During daytime we expect $d1231 = +0.04 \pm 0.06 \text{ K}$, since the $0.17 \pm 0.03 \text{ K}$ cold skin bias is almost offset by the fact that during the day the RTGSST is $0.21 \pm 0.05 \text{ K}$ colder than the buoys. The results from tropical ocean daytime data are summarized in Table 2 for three filters, cx2616 = 0.7 K, the nominal cx2616 = 0.5 K, and cx2616 = 0.5 K with vis3 < 5 added. The third column in Table 2 shows d1231, and the fifth column shows the observed signal in vis3. Under perfectly clear conditions we expected $\text{vis3} = 4$ and $d1231 = +0.04 \pm 0.06 \text{ K}$. As the spatial coherence threshold is tightened from cx2616 = 0.7 K to the nominal cx2616 = 0.5 K threshold, the mean vis3 value decreases slightly from 6.8 to 6.6 and the d1231 values changes from -0.22 K to -0.20 K . This is the first indication of cloud effects, and that they are lessened by tighter filtering. This data set typically contains 3000 footprints per day. If the (vis3 < 5) condition is added to the cx2616 < 0.5K threshold (bottom row in Table 2), 750 footprints per day pass (0.1% of all footprints) and $d1231 = +0.10 \text{ K}$. During the day we expected $d1231 = 0.04 \text{ K}$, only 0.06 K less than the observed value. We conclude that the cloud contamination of sst1231 using the cx2616 = 0.5 K cloud filter alone is $-0.20 - 0.10 + 0.04 = -0.26 \text{ K}$.

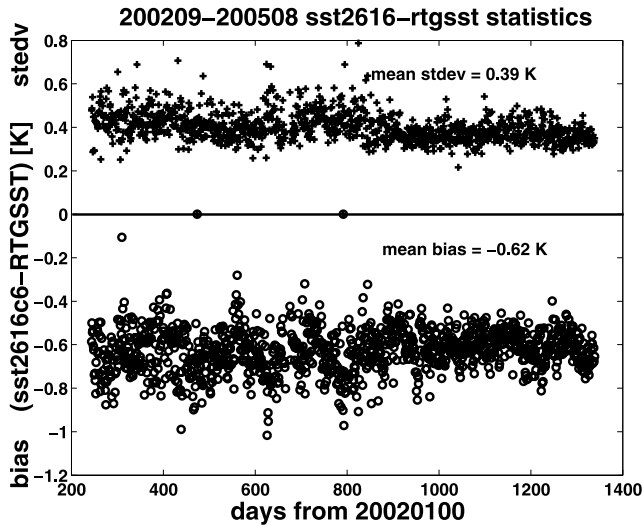


Figure 3. Three years of clear night tropical ocean (sst2616 – RTGSST), showing a cold bias (bottom), but a small standard deviation (top). The change in the character of the standard deviation and the tighter bias starting on day 859 correspond to the upgrade of the RTGSST software in May 2004.

[26] In order to estimate the day/night bias and the cloud contamination bias, we used daytime clear data, and assumed that the cloud filter removes night clouds and day clouds with equal efficiency; that is, the cold bias in sst1231 due to the cloud contamination day and night is the same. The argument for this assumption is as follows: During the day under $cx2616 < 0.5$ K conditions we expected $d1231 = +0.04 \pm 0.06$ K and measured -0.20 K, i.e., a 0.24 K cold bias due to cloud contamination. At night we expected a bias of $-0.17 - 0.17 = -0.34$ K, but we measured -0.59 K, i.e., 0.25 K colder owing to cloud contamination. The close agreement between the daytime and the nighttime estimates of cloud contamination and the estimated cloud contamination during daytime using the vis3 filter show that the assumed day/night balance of the cloud filter is true.

[27] The above evaluation pertains to the cold bias from cloud contamination in sst1231. Because of the nonlinearity of the Planck function, a given fractional cloud cover affects sst2616 less than sst1231. We evaluate the magnitude of this effect using a simple cloud contamination model, where the cloud fraction is deduced from the vis3 signal. $Vis3 = 6.6$ corresponds to an approximate fractional cloud cover of $(6.6 - 4)/260 = 1\%$. This fraction of the area of the AIRS footprint is covered with clouds, the rest of the footprint sees the 300 K surface. This model is consistent with the observed cold bias in sst1231 assuming a 260 K cloud top temperature, and results in a 0.20 K cold bias for sst2616, i.e., 0.08 K less than for sst1231.

[28] Given that we observed 0.26 K from sst1231, deduced 0.25 K from the night observations, and calculated a 0.2 K bias for sst2616 from the cloud contamination model, we use the difference between the maximum and the minimum as an estimate of the bias uncertainty; that is, the

estimated cloud contamination bias at 2616 cm^{-1} is 0.25 ± 0.06 K.

2.6. Summary of Expected Systematic Night Bias and Bias Uncertainties

[29] The following potential biases and RMS bias uncertainties need to be included in the final analysis of the night (obs-calc) at 2616 cm^{-1} : (1) atmospheric transmission, -0.04 ± 0.08 K; (2) sea surface emissivity, 0 ± 0.03 K; (3) skin-bulk conversion, -0.17 ± 0.03 K; (4) night bias correction, -0.17 ± 0.05 K; and (5) cloud contamination, -0.25 ± 0.06 K.

[30] It is interesting to note that in spite of the extremely high transparency of the 2616 cm^{-1} window channel, the 0.08 K uncertainty in the transmission correction is the largest individual component in the overall bias uncertainty, closely followed by the uncertainty in bias due to cloud contamination. The individual bias estimates add, and the bias uncertainties combine as root sum squared (rss). Including cloud contamination the expected bias of (obs-calc) is -0.63 ± 0.12 K. The radiometric calibration bias is then given by the difference between the observed bias and the expected bias.

3. Results and Discussion

[31] In the discussion of the results for (obs-calc) we use the more intuitive, but numerically equivalent sst2616 – RTGSST. Figure 3 shows the results for 3 years of RTGSST matchups, from 1 September 2002, when AIRS started to produce data in the operational mode, through 31 August 2005. Each point in Figure 3 represents the mean of about 4000 matchups from the descending (night) orbits; the daily median is plotted in the bottom panel, the daily standard deviation is plotted in the top panel. In May 2004 the RTGSST software was upgraded, resulting in a noticeable decrease in the standard deviation and a small shift in the median. The median of (sst2616 – RTGSST) changed from -0.64 K to -0.60 K, while the standard deviation decreased from 0.42 K to 0.37 K. The first impression of Figure 3 is that for the past 3 years the sst2616 from the tropical oceans has tracked the RTGSST remarkably well, albeit with a significant, but statistically very stable cold bias. In the following we discuss the daily bias, the daily mean standard deviation and the trend in the bias.

3.1. Bias in (obs-calc)

[32] We expect a bias between sst2616 and the bulk SST, -0.17 K (skin) and -0.17 K (day/night), we identified a small bias in the RTA, -0.04 K, and we found an unexpected cloud contamination, -0.25 K, resulting in a combined bias of -0.63 ± 0.12 K. The observed 3 year mean bias was -0.62 K (-0.64 K before and -0.60 K after May 2004). The difference between the expected and the observed bias is 10 ± 120 mK. This result is consistent with the prelaunch estimate of the calibration accuracy for 300 K scenes of 48 mK based on the effective OBC emissivity uncertainty. On the basis of the 120 mK uncertainty in the bias correction, we conclude that the AIRS absolute radiometric calibration at 2616 cm^{-1} has been validated within 200 mK. While the 200 mK performance was demonstrated only for the 2616 cm^{-1} measurements of tropical ocean

temperatures, i.e., 295 K–305 K, the AIRS design virtually assures similar performance for all channels for the same temperature range. *Tobin et al.* [2004] used under-flights of AIRS in November 2002 to validate the AIRS radiances between 700 and 1500 cm^{-1} at the 200 mK level for temperatures between 250 K and 300 K. *Walden et al.* [2006] used surface observations at Dome Concordia in January 2003 and January 2004 to demonstrate absolute calibration accuracy within 200 mK in same spectral region, but for temperatures between 230 and 250 K.

3.2. Standard Deviation of (obs-calc)

[33] The standard deviation of (obs-calc) is due to the combination of the random error in sst2616 and the random error in the RTGSST. The mean daily standard deviation of sst2616 – RTGSST was 0.42 K before May 2004, and improved to 0.37 K afterward. In the following we discuss only the more recent 0.37 K value.

[34] 1. The typical rmsd derived by NCEP from the comparison of the RTGSST with the held-back verification buoys is 0.45 K rmsd. Since the difference between the buoys and the RTGSST is zero mean, rmsd and standard deviation are identical.

[35] 2. The random component in sst2616 is due to the combination of the calculation noise and the pseudo-random noise introduced by the leak in the cloud filter. The calculation noise in sst2616 is the result of the weighted NeDT of the 2616 cm^{-1} and the 2607 cm^{-1} channels combined with 0.05 K RMS of the water vapor correction. The resulting calculation noise in sst2616 is 0.1K. This is the minimum random noise, since the presence of undetected clouds contamination in the clear data must itself have a random component. The data passed by any cloud filter contain some totally cloud-free footprints (extremely infrequent), there is a mean cold bias, in our case 0.25 K for tropical oceans, but half the footprints passed as clear will have cloud contamination larger than the mean. This suggests that the cloud leak follows an exponential distribution. For the case of a simple exponential distribution the standard deviation equals the mean. With this assumption we could have 0.25 K of cloud filter noise. The effective noise in sst2616 is clearly larger than 0.1K, possibly as large as 0.27 K.

[36] The fact that the observed 0.37 K standard deviation for (sst2616 – RTGSST) is already less than the claimed rmsd of the RTGSST relative to the buoys appears to be inconsistent. This inconsistency is made worse by the fact that sst2616 itself includes a random component larger than 0.1K. The most likely explanation is that the AIRS IR measurements and RTGSST data are indirectly correlated. The RTGSST is derived from buoys, but the interpolation includes the AVHRR SST, which is derived by regression of IR window measurements relative to the buoys. The areas that AIRS identified as extremely clear are filled by a large number of high-quality AVHRR SST measurements. So it should not be too surprising that the AIRS sst2616 and the RTGSST in these areas are in better agreement than the agreement of the RTGSST with buoys in all of the tropical oceans, most of which are cloudy. This argument also suggests that the reason for the significant decrease in the standard deviation of (sst2616 – RTGSST) after the May

2004 RTGSST software upgrade is directly or indirectly a tighter coupling of the RTGSST to infrared measurements.

3.3. Trend in (obs-calc)

[37] The change in the RTGSST software in May 2004 complicates the 3 year trend analysis of (obs-calc). The trend changed from -5 ± 8 mK/yr before the change to -18 ± 8 mK/yr after May 2004. With only 3 years of data, with an RTGSST software change in the middle, it is difficult to decide what the stability of the 2616 cm^{-1} radiances themselves might be. A reasonably safe estimate of the stability of the AIRS 2616 cm^{-1} calibration as better than 16 mK/yr, twice the standard deviation of trend uncertainties derived from (obs-calc). Given that 0.25 K of the bias is due to cloud contamination in spite of very tight cloud filtering, a significant fraction of the observed trend may in fact be due to interannual variability of convective activity, which gives rise to variability in the clouds which slip through the AIRS cloud filter. However, the estimated upper limit of 16 mK/yr radiometric stability is already adequate for the evaluation of some expected trends. As an example, the brightness temperature of the 2388 cm^{-1} CO₂ R-branch channel will decrease at the rate of 75 mK/yr in response to the increase in the CO₂ column abundance of 2 ppmv/yr.

[38] The stability of the bias (sst2616 – RTGSST) largely confirms the stability of the OBC output. While the common use of the OBC goes a long way toward ensuring the stability of all AIRS channels at a level comparable to that derived for 2616 cm^{-1} channel, second-order effects due to component aging and contamination during the anticipated 7 year on-orbit life will require additional analysis.

4. Summary and Conclusions

[39] The excellent absolute radiometric accuracy and stability expected from the cooled grating-array spectrometer design of AIRS and confirmed during prelaunch testing, has been verified using the first 3 years of AIRS data. The comparison of the observed brightness temperatures and those calculated at TOA from the RTGSST validates the absolute accuracy of the 2616 cm^{-1} radiances to better than 200 mK and the stability to better than 16 mK/yr for the first 3 years of AIRS data. This result validates the accuracy and stability of the On-Board Blackbody Calibrator (OBC) and the ground-based calibration software. The limitations to the validation of the absolute accuracy of the AIRS radiances to significantly better than 200 mK is not the absolute accuracy of the RTGSST, but the uncertainty in the estimated atmospheric transmission and the residual cloud contamination.

[40] Since the stability and accuracy demonstrated at 2616 cm^{-1} basically establishes the accuracy and stability of the OBC, which is used by all channels, the grating-array spectrometer design virtually ensures the comparable absolute calibration accuracy and stability for all channels. The better than 16 mK/yr stability sets a benchmark of what can be achieved with a state-of-the-art hyperspectral radiometer from polar orbit and what is expected from future hyperspectral sounders. With a nominal lifetime of 7 years of absolutely calibrated hyperspectral resolution data, AIRS will measure temperature and trends in the state of the

atmosphere for the 2002–2009 time period. This data record may be continued by the next generation of hyperspectral sounders in the form of IASI (launch expected in 2006) and CRIS (NPP launch no sooner than 2008). Sea surface temperatures will provide the common benchmark.

Appendix A: sst2616 and sst1231

[41] Following are the algorithms for sst2616v24s and sst1231r5 in Matlab vector notation. The % in the first column indicates a comment.

[42] % sst2616v24s

[43] % The szas is the array of the local satellite zenith angle in degrees.

[44] % First we set up the Masuda emissivity as an array matching bt2616s.

[45] e2616 = ones(size(bt2616s)); v25 = find(abs(szas) > 25);

[46] e2616(v25) = (cos((abs(szas(v25)) - 25) * 0.6 / 57.3)).^0.4; % Masuda v = 5 m/sec

[47] % Calculate the transmission correction for e = 1.0 in temperature domain

[48] % the coefficients are based on Jan2003 RTA trained on 24 profiles at

[49] % sza = [0,10,20,20,40,50].

[50] q2 = bt2616s - bt2607s;

[51] a2616 = 0.109 + 0.0432 * q2 + 0.00689 * (q2.^2);

[52] % the emissivity correction is done in radiance domain

[53] sst2616v24s = btemp(2616, planck(2616, bt2616s + a2616) / (0.976 * e2616));

[54] % planck(nu, T) and btemp(nu, rad) are the Planck function and its inverse

[55] % for night abs(lat) < 30 degree abs(szas) < 35 degree ocean cx2616 < 0.5 on 20050422

[56] % (sst2616c24(v05n) - rtgs(v05n)) = -0.676 ± 0.371 for 9324 pts

[57] % sst1231r5s

[58] q3 = bt1231s - bt1227s;

[59] % sst1231r5s regressed on sst2616c6s at night using 200310 data

[60] % filtered with cx2616 < 0.5K

[61] sst1231r5s = bt1231s + 0.2806 + 1.2008 * q3 + 0.2962 * q3.^2 + 1.0489 ./ cos(szas/57.3);

[62] % for night abs(lat) < 30 degree abs(szas) < 35 degree ocean cx2616 < 0.5 on 20050422

[63] % (sst1231r5s(v05n) - rtgs(v05n)) = -0.665 ± 0.428 for 9324 pts

[64] % note that sst2616v24s and sst1231r5s are biased within 10 mK relative to the RTGSST

[65] % but sst1231r5s has a significantly larger standard deviation relative to RTGSST.

[66] **Acknowledgments.** The AIRS instrument design concept was developed by the JPL Team under Fred O'Callaghan and implemented by the BAE Team under Jerry Bates and Paul Morse, with Chris Miller's system analysis. Ken Overoye from BAE, who designed most of the ground-calibration system, and Tom Pagano, who lead the calibration team

at JPL, deserve much of the credit for the exceptional calibration accuracy of AIRS. This work was carried out at the Jet Propulsion Laboratory, California Institute of Technology, under contract with NASA.

References

- Aumann, H. H. (2003), Results from the Atmospheric Infrared Sounder (AIRS) on the EOS Aqua one year after launch, paper 5234-14 presented at SPIE 10th International Symposium Remote Sensing, Barcelona, Spain, 8–12 Sept.
- Aumann, H. H., et al. (2003), AIRS/AMSU/HSB on the Aqua Mission: Design, science objectives, data products and processing systems, *IEEE Trans. Geosci. Remote Sens.*, **41**, 253–264.
- Aumann, H. H., D. Gregorich, and D. Barron (2004), Spectral cloud-screening of AIRS data: Non polar ocean, paper presented at 49th Annual Meeting on Optical Science and Technology, Int. Soc. for Opt. Eng., Denver, Colo., 2–6 Aug.
- Chahine, M. T. (1981), Remote sensing of sea-surface temperature in the 3.7 μm CO₂ Band, in *Oceanography from Space*, edited by J. F. R. Gower, pp. 87–95, Springer, New York.
- Coakley, J. A., and F. P. Bretherton (1982), Cloud cover from high resolution scanner data: Detecting and allowing for partially filled fields of view, *J. Geophys. Res.*, **87**, 4917–4932.
- Donlon, C. J., P. J. Minnett, C. Gentemann, T. J. Nightingale, I. J. Barton, B. Ward, and M. J. Murray (2002), Toward improved validation of satellite sea surface skin temperature measurements for climate research, *J. Clim.*, **15**, 353–369.
- Gautier, C., Y. Shiren, and M. D. Hofstadter (2003), AIRS/Vis near IR instrument, *IEEE Trans. Geosci. Remote Sens.*, **41**, 330–342.
- Hagan, D. E., and P. J. Minnett (2003), AIRS radiance validation over oceans from sea surface temperature measurements, *IEEE Trans. Geosci. Remote Sens.*, **41**, 432–441.
- Lambertsen, B. H. (2003), Calibration of the AIRS Microwave Instruments, *IEEE Trans. Geosci. Remote Sens.*, **41**, 369–378.
- Masuda, K., T. Takahima, and Y. Takayama (1988), Emissivity of pure and sea water from the model sea surface in the infrared window regions, *Remote Sens. Environ.*, **24**, 313–329.
- Minnett, P. J., R. O. Knuteson, F. A. Best, B. J. Osborne, J. A. Hanafin, and O. B. Brown (2001), The Marine-Atmospheric Emitted Radiance Interferometer (MAERI): A high accuracy, sea-going infrared spectroradiometer, *J. Atmos. Oceanic Technol.*, **28**, 994–1013.
- Pagano, T. S., H. H. Aumann, D. Hagan, and K. Overoye (2003), Prelaunch and in-flight radiometric calibration of the Atmospheric Infrared Sounder (AIRS), *IEEE Trans. Geosci. Remote Sens.*, **41**, 265–273.
- Reynolds, R. W., N. A. Rayner, T. M. Smith, D. C. Stokes, and W. Wang (2002), An improved in situ and satellite SST analysis for climate, *J. Clim.*, **15**, 1609–1625.
- Strow, L., S. Hannon, S. DeSouza Machado, H. Motteler, and D. Tobin (2003), An overview of the AIRS radiative transfer model, *IEEE Trans. Geosci. Remote Sens.*, **41**, 303–313.
- Strow, L. L., S. E. Hannon, S. DeSouza Machado, H. E. Motteler, and D. C. Tobin (2006), Validation of the Atmospheric Infrared Sounder radiative transfer algorithm, *J. Geophys. Res.*, **111**, D09S06, doi:10.1029/2005JD006146.
- Thiébaux, J., E. Rogers, W. Wang, and B. Katz (2003), A new high-resolution blended real-time global sea surface temperature analysis, *Bull. Am. Meteorol. Soc.*, **84**(5), 645–656.
- Tobin, D., et al. (2004), Validation of Atmospheric Infrared Sounder (AIRS) spectral radiances with the scanning high-resolution interferometer sounder (S-HIS) aircraft instrument, *Opt. Eng.*, **55**(7), doi:10.1117/12.566060.
- Walden, V. P., W. L. Roth, R. S. Stone, and B. Halter (2006), Radiometric validation of the Atmospheric Infrared Sounder over the Antarctic Plateau, *J. Geophys. Res.*, **111**, D09S03, doi:10.1029/2005JD006357.
- Weller, R. A., and S. P. Anderson (1996), Surface meteorology and air-sea fluxes in the western equatorial Pacific warm pool during the TOGA Coupled Ocean Atmosphere Response experiment, *J. Clim.*, **9**, 1959–1990.

H. H. Aumann, S. Broberg, D. Elliott, S. Gaiser, and D. Gregorich, Jet Propulsion Laboratory, California Institute of Technology, Pasadena, CA 91109, USA. (aumann@jpl.nasa.gov)